From Back to Front: A Functional Model for the Cerebellar Modulation in the Establishment of Conditioned Preferences for Cocaine-Related Cues

Isis Gil-Miravet M.S[1], Ignasi Melchor-Eixea M.S[1], Edgar Arias-Sandoval M.S[1], Lizbeth Vasquez-Celaya Ph.D[3], Julián Guarque-Chabrera M.S[1], Francisco Olucha-Bordonau Ph.D[2], Marta Miquel Ph.D[1]*

1 Área de Psicobiología, Universitat Jaume I, Castellón de la Plana, Spain.

2 UP Medicina. Universitat Jaume I, Castellón de la Plana, Spain.

3 Centro de Investigaciones Cerebrales. Universidad Veracruzana, Xalapa, Mexico.

*Corresponding author. Área de Psicobiología, Universitat Jaume I, Avenida Vicente Sos Baynat sn, 12071, Castellón de la Plana, Spain.

miquel@uji.es

orcid.org/0000-0001-9670-4210

Running title: Cerebellar modulation of cocaine-induced memory

ABSTRACT

It is now increasingly clear that the cerebellum may modulate brain functions altered in drug addiction. We previously demonstrated that cocaine-induced conditioned preference increased activity at the dorsal posterior cerebellar vermis. Unexpectedly, a neurotoxic lesion at this region increased the probability of cocaine-induced conditioned preference acquisition. The present research aimed at providing an explanatory model for such as facilitative effect of the cerebellar lesion. First, we addressed a tracing study in which we found a direct projection from the lateral (dentate) nucleus to the VTA that also receives Purkinje axons from lobule VIII in the vermis. This pathway might control the activity and plasticity of the cortico-striatal circuitry. Then, we evaluated cFos expression in different regions of the medial prefrontal cortex and striatum after a lesion in lobule VIII before conditioning. Additionally, perineuronal net (PNN) expression was assessed to explore whether the cerebellar lesion might affect synaptic stabilization mechanisms in the medial prefrontal cortex (mPFC). Damage in this region of the vermis induced general disinhibition of the mPFC and striatal subdivisions that receive dopaminergic projections, mainly from the ventral tegmental area (VTA). Moreover, cerebellar impairment induced an upregulation of PNN expression in the mPFC. The major finding of this research was to provide an explanatory model for the function of the posterior cerebellar vermis on drug-related memory. In this model, damage of the posterior vermis would release striatum-cortical networks from the inhibitory tonic control exerted by the cerebellar cortex over VTA, thereby promoting drug effects.

Keywords: cocaine, cerebellum, quinolinic acid, PNNs, VTA

INTRODUCTION

For decades, the cerebellum's role has been viewed to be restricted only to motor functions. However, numerous investigations in the last decades have described the involvement of the cerebellum in non-motor functions including language, spatial and emotional processing, reward, working memory, and executive functions (1-9). Anatomical and functional studies in rodents and non-human primates have shown extensive pathways that connect the cerebellum to the prefrontal cortex, striatum, amygdala, thalamus, hippocampus, and basal ganglia (10-21). More recently, two findings pointed to a direct control of the cerebellum over the VTA (9, 22). All these results suggest that the cerebellum is part of cortical-striatal-limbic loops and may modulate brain functions that might be altered in drug addiction (23-25).

Indeed, the cerebellum plays an important role in the consolidation of non-motor Pavlovian memory and in the establishment of automatic behavioral protocols (4, 26). Moreover, neuroimaging studies of drug-induced cue reactivity in drug addicts described cerebellar activation after the presentation of drug-related cues (27-32). In a mice model of cocaine-induced conditioned preference, we showed that only those animals that developed preference for cocaine-related cues exhibited increased activity at the apical region of the cerebellar vermis (33-35). Although this effect was found throughout the cerebellar cortex, only activity in lobule VIII was significantly correlated with the level of preference towards cocaine-related cues (34). Furthermore, cocaine-induced conditioned preference also increased the expression of PNNs surrounding Golgi inhibitory interneurons located in the same region of the vermis (35), suggesting that drug-induced Pavlovian memory encouraged one of the main mechanisms for synaptic stabilization (36). On that basis, it could be expected a neurotoxic lesion localized in lobule VIII may prevent the acquisition of cocaine-induced conditioned preference. On

the contrary, the cerebellar lesion dramatically raised by up to 100 the percentage of rats that acquired cocaine-induced conditioned preference (37). The same effect was observed after a reversible deactivation of the infralimbic (IL) cortex (37). Moreover, simultaneous IL-cerebellar deactivation prevented the effect of either of the separate manipulations (37). These results were in agreement with findings reporting that the IL cortex is required for the suppression of cocaine-seeking response and expression of extinction memory (38, 39). Overall, our findings suggested that both the cerebellum and IL cortex might act together in regulating the establishment of drug-cue Pavlovian associations.

The present research aimed at: (1) further investigating cerebellum-infralimbic functional relationships for the acquisition of cocaine-induced conditioned preference; and (2) proposing a functional model to explain the effects of the cerebellar lesion in cocaine-conditioned memory. First, we addressed a tracing study using anterograde and retrograde tracers in order to build a working neuroanatomical model to explain our prior findings. Second, we assessed cFos expression in different regions of the medial prefrontal cortex and striatum after the neurotoxic lesion in the apical region of lobule VIII before conditioning. Finally, we explored if the cerebellar lesion might affect synaptic stabilization mechanisms through PNN expression in the medial prefrontal cortex.

METHODOLOGY

Subjects

Twenty-two male Sprague-Dawley rats (Janvier, ST Berthevin Cedex, France) weighing between 175 and 200 g were individually housed under standard laboratory conditions, with controlled temperature and humidity (12-hour light cycle from 8:00 a.m. to 8:00 p.m.) and access to food and water ad libitum (Jaume I University, Spain). Rats were

handled and habituated to all of the experimental procedures. All animal procedures were approved by the local Animal Welfare Ethics Committee and Empowered Body (2014/VSC/PEA/00208) and developed in accordance with the European Community Council Directive (2010/63/EU), Spanish directive BOE 34/11370/2013, and local directive DOGV 26/2010.

Brain infusions and stereotactic surgery

The animals were anesthetized using a cocktail of ketamine (100 mg/kg) (Imalgene 100 mg/ml, Mersal Laboratorios S.A., Barcelona, Spain) and xylazine (10 mg/kg) (Xylazine hydrochloride ≥99%, Sigma-Aldrich, Madrid, Spain) (IP), and placed in a Kopf stereotaxic apparatus for the surgery. We use a stainless-steel guide cannula (10 mm length; 23-gauge external diameter) for the intracranial infusions. Infusions were released through a removable stainless-steel injector (length, 11 mm; external diameter, 30-gauge) inserted into the previously implanted guide cannula.

For the anatomic study, retrograde and anterograde tracers were infused in different regions of the brain. As a retrograde tracer, we used FluoroGold with DAPI (FG) (5-hydroxystilbamidine, Cat# 80014, Biotium, Hayward, CA) dissolved at 4% in destillated water. The anterograde tracing was accomplished using Biotinilated Dextranamine (BDA, 10,000 MW, Lysine Fixable, Cat# D1956, Molecular Probes, Eugene, OR) dissolved at 10% in PB 0.1M pH 7.4. The following coordinates were used: IL (AP: +3.2; ML: + 0.6/−0.6; DV: −5); VTA (AP: -5.2; ML: + 0.9/−0.9; DV: −8.3); lateral nucleus (Lat) (AP: -11.4; ML: + 3.6/−3.6; DV: −6.2); interpositus nucleus, anterior part (IntA) (AP: -11.3; ML: + 2.5/−2.5; DV: −5.8), posterior part (IntP) (AP: -11.7; ML: + 2.5/−2.5; DV: −6.2); medial nucleus (Med) (AP: -11.4; ML: + 1/−1; DV: −6.2); and the apical area of lobe VIII in the vermis (AP: −14.5; ML: 0; DV: −4.5) [40]. FG or BDA infusion

volumes were 0.5 µL in the IL and 0.3 µL in the rest of regions with an infusion ratio of 0.2 µL /min. After infusions, the rats remained undisturbed for ten days before perfusion.

Quinolinic acid (QA) (90 nmol/µL) (2,3-Pyridinedicarboxylic acid, Sigma-Aldrich, Madrid, Spain) dissolved in phosphate buffered saline (PBS; 0.1 M pH 7.4) and infused into the dorsal region of lobe VIII in the vermis (0.5 µL volume; infusion ratio of 0.2 µL/min) (AP: −14.5; ML: 0; DV: −4.5) (40). After infusion, the cannula remained in place for three minutes to allow for diffusion. The same procedure was implemented in the sham group by infusing PBS. After the surgery, all the animals received analgesic treatment with meloxicam (Metacam: 2 mg/kg, 5 mg/mL, Boehringer Ingelheim, Barcelona, Spain) for 24 hours for three days. Cannula locations were verified by Nissl immunostaining and camera lucida (Fig 1A). More detailed information can be found in (37).

Cocaine-induced preference conditioning procedure

The cocaine-induced conditioning procedure has been published previously (37). Briefly, conditioning was conducted using two equally preferred olfactory stimuli located in the walls of a black chamber (20 × 20 × 60 cm) at the opposite arms of a corridor. One of the odors acted as the conditioned stimulus (CS+) and was associated with an IP injection of cocaine hydrochloride (15 mg/kg, IP) (Alcaliber S.A., Madrid, Spain). On alternate days, rats were exposed to the other scent (CS−) placed at the opposite black chamber in the corridor and received 0.9% saline injections. During pairing sessions (15 minutes) animals remained confined in the chamber. A total of eight cocaine-paired sessions were conducted. The olfactory cues and locations in the corridor were counterbalanced between animals. Preference for the cocaine-related cue was evaluated 48 hours after the last cocaine administration in a 30-minute, drug-free test in which CS+ and CS− odors were present simultaneously but in opposite arms of the corridor. The first ten minutes

were not considered in order to allow the animal to explore the location of the odors, which was the opposite to the conditioning phase. The preference score was calculated as [Time Spent in CS+ / (Time Spent in CS+ + Time Spent in CS−)] × 100. Additionally, we included a pseudo-conditioning group (the Unp group) that was treated with the same number of cocaine injections but randomly associated with the olfactory stimuli. The Unp group allowed us to test for memory-related effects of our brain deactivations. Animals were perfused transcardially 90 minutes following the preference test. For perfusion, animals were deeply anesthetized and euthanized with an overdose of Nembutal (150 mg/kg, i.p. Euthalender, Normon, Barcelona, Spain) and perfused by transcardial infusion with saline (250 ml) and fixative solution (4% formaldehyde in 0.1 M PB, pH 7.4). Brains were removed from the skull, postfixed in fixative solution overnight at 4ºC and cryoprotected in 30% sucrose in 0.01 M PBS, pH 7.4.

Immunohistochemistry and immunofluorescence

The brain tissue was frozen with liquid nitrogen, and sections were performed at 40 μm with a cryostat microtome (Microm HM560, Thermo Fisher Scientific, Barcelona, Spain). Eight series of tissue sections were collected and stored at −80 °C in a cryoprotectant solution.

Immunolabeling was performed on free-floating sections. For cFos peroxidative immunostaining, tissue peroxidases were eliminated, and the brain tissue was incubated for 48 hours with a polyclonal primary antibody, rabbit anti-cFos (1:1000; Synaptic Systems, Goettingen, Germany), and then, for 120 minutes with an affinity purified secondary biotinylated antibody, goat anti-rabbit (1:400; Jackson InmunoResearch Laboratories, Inc., West Grove, PA, USA). For amplification, we used preassembled biotin–avidin peroxidase complex according to the Vector Labs recommendations (ABC Elite; Vector Laboratories, Bulingame, Ca, USA). Sections were exposed to a DAB

solution with nickel (Vector Laboratories, Bulingame, Ca, USA). Then the tissue was rinsed and mounted in Eukitt (Sigma-Aldrich, Madrid, Spain). For PNN analysis, fluorescence immunolabeling for Wisteria Floribunda Agglutinin (WFA), cFos, and parvalbumin (PRV) were used. Brain tissue was incubated with lectin from WFA (1:200; Sigma-Aldrich, Madrid, Spain), the polyclonal primary antibody, rabbit anti-cFos (1:1000; Synaptic Systems, Goettingen, Germany), and **polyclonal** mouse anti-PRV (1:15,000; Swant, Switzerland) at 4.0 °C for 48 hours in PBS 0.1M triton X-100 (PBST). In a second step, brain samples were exposed to FICT-Streptavidin (1:50; Jackson InmunoResearch Laboratories, Inc., West Grove, PA, USA) and goat anti-rabbit Cy5 (1:200; Jackson InmunoResearch Laboratories, Inc., West Grove, PA, USA). VTA-DA projections were identified by Tyrosine Hydroxylase immunofluorescence (TH) (1:500; sheep anti-TH; Thermo Fisher Scientific, Rockford, IL, USA), and dopamine transporter immunolabelling (DAT) (1:200; rabbit anti-DAT; Bioss antibodies, Boston, Massachusetts, USA) was used to estimate dopaminergic activity in the mPFC. The anterograde tracer BDA was revealed by Cy3-conjugated Streptavidin (1:300; Jackson InmunoResearch Laboratories, Inc., West Grove, PA, USA). Immunolabeling for GABA vesicular transporter (VGAT) (1:100, polyclonal guinea pig anti-VGAT; Synaptic Systems, Goettingen, Germany), vesicular glutamate transporters (VGLUT2) (1:500, polyclonal guinea pig anti-VGLUT2; Synaptic Systems, Goettingen, Germany) and synapsin 1 (SYN) (1:200; mouse monoclonal anti-Syn 1; Synaptic Systems, Goettingen, Germany) was conducted to better describe synaptic contacts within the lateral nucleus and VTA in the anatomical study. All the sections were mounted with Mowiol (Calbiochem, EMD Chemicals, Inc, San Diego CA, USA).

Image acquisition and analysis

Fluorescent images of the infusion locations and tracer diffusion were acquired as eight confocal stacked images using the tile-scan tool (Leica DMi8, Leica Microsystems CMS GmbH, Wetzlar, Germany) in order to obtain complete coronal sections in which ROIs were presented.

Images of immunoperoxidase cFos expression were acquired using an optic microscope (Nikon E-800, Izasa Werfen Group, Valencia, Spain) with 20x lenses and a resolution of 1,360 x 1,024 dpi. Three photos were taken by structure: Infralimbic (IL), Prelimbic (PL), dorsomedial striatum (DMS), dorsolateral striatum (DLS), ventrolateral striatum (VLS), nucleus accumbens core (NAcC) and shell (NAcSh)), and hemisphere in coronal sections. We included bregma coordinates between 3.20 mm to 2.20 mm for PL and IL, and for the striatum and NAc between 1.60 mm to 0.70 mm.

Fluorescence images of cFos and PNNs were captured in the above-mentioned confocal microscope with 20x lenses and resolution 1,024 x 1,024 dpi Laser intensity (1.0%), gain (600) and offset (-4) remained constant in each analysis. Each image was formed by a stack of ten images. Image stacks were pre-processed applying a maximal projection process with Leica Application Suite LAS X (Leica Microsystems CMS GmbH, Wetzlar, Germany). Three image stacks in coronal sections for brain regions and in sagittal sections for deep cerebellar nuclei were acquired by structure and hemisphere.

FIJI free software (41) was used for all quantifications. Unmodified images were used in all analyses. cFos expression was evaluated using the cell-counter plug-in of FIJI software. Additionally, PNN expression was estimated using a densitometry assessment of WFA intensity (brightness range 0-255) in all the PNNs that were found in three sections of each ROI (35, 42, 43).

Experimental design and statistics

All statistical analyses were performed using GraphPad Prism 7 software (GraphPad Software Inc., La Jolla, CA, USA). One-way ANOVAs and Student t-tests for independent samples were carried out as parametric tests. Individual scores were provided for each variable. In addition, data were presented as mean ±SEM. Post hoc comparisons were performed using Tukey's HSD tests. The statistical level of significance was set at $p < 0.05$. When non-parametric statistics was required Kruskal-Wallis and Mann-Whitney-Wilcoxon tests were conducted and data were represented as the median.

RESULTS

Cocaine-induced conditioned preference

In an earlier study, we showed that an excitotoxic lesion in the apical region (dorsal) of lobule VIII before conditioning facilitated cocaine-induced conditioned preference (37). Indeed, the whole sample of lesioned animals developed a preference for the cocaine-related cue, as compared to only one third of the sham group. In the present study, we confirmed the results with the smaller sample of rats in which immunohistochemical studies were conducted (N=18) [the sham group (n = 6), the lesioned group (QA) (n = 6), and the pseudo-conditioned group (Unp) (n = 6)]. As expected, the cerebellar lesion promoted the acquisition of cocaine-induced conditioned preference [$F(2,15) = 5.34$, $p = 0.0178$]. Post hoc analysis revealed that the QA group showed significant higher preference that the sham ($p = 0.0463$) and Unp ($p = 0.0235$) groups. Remarkably, no difference was found between the sham and Unp groups ($P = 0.9350$). Therefore, the

neurotoxic lesion was ineffective in affecting the behavior of the Unp group, indicating that lesion effects were learning-related (Fig S1).

Anterograde and retrograde tracing

To propose a working neuroanatomical model that may explain behavioral effects of the lesion in the posterior vermis (37), we carried out an anatomical study using anterograde (BDA/red) and retrograde (FG/blue) tracers. Very recent findings pointed to a direct control of the cerebellum over the ventral tegmental area (9). Therefore, BDA was infused into the apical region of lobule VIII in the vermis (the same location as the excitotoxic lesion) and the Lat nucleus. In turn, we infused FG into the VTA and IL cortex. We searched for colocalization between BDA and FG within the VTA and Lat nucleus (n = 3) (Figs 1-2; S2-S3).

Despite the fact that the infusion point was restricted to lobule VIII in the vermis, BDA-labeled projections were found throughout the whole vermis, but also the hemispheres, reaching Crus I (Fig. 1). However, the molecular layer along the cerebellar cortex was devoid of BDA labeling. BDA is an anterograde tracer that identifies only a neural projection from their source to their point of termination. Hence, one plausible explanation for these results is that Purkinje-to-Purkinje collaterals would have spread the tracer laterally from the middle line along the cerebellar cortex. Purkinje collateral branches originated within the parasagittal plane can reach 2.0 mm towards the apex of the granule cell layer and the base of the lobule in adult rodents (44). Importantly, these findings suggested that lobule VIII in the vermis might be interconnected with distal regions in the cerebellar cortex. As expected, we observed a great number of BDA-labeled terminals within **the deep cerebellar nuclei (DCN),** especially within the medial nucleus, but also in the IntA; IntP and Lat nuclei (Fig. 1).

When infusing FG into the VTA, FG-labeled somata were found within the contralateral IntA, IntP, and Lat, but not in the Med (Fig. 1). We also observed some FG+ somata in mPFC and NAcSh, among other already described afferences to VTA, what replicated the results observed in other studies (45, 46). Then, this cerebellar afference to VTA was confirmed by infusing BDA into the Lat nucleus (Fig. 2). Unilateral BDA infusions into the Lat nucleus reached ipsilateral cerebellar hemisphere, lobule VIII and IX of the vermis, and contralateral parabrachial pigmented nucleus of the VTA (PBP), the most caudal part of the VTA (Fig. 2). At higher magnifications it was possible to observe in the Lat close putative contacts between Purkinje BDA+ terminals from lobule VIII and FG+ cerebellar cells retrogradely labeled from VTA tracer injection (Fig 1).

Additionally, by infusing FG in the IL cortex and BDA in the Lat (n = 2), we observed close apposition between anterogradely labeled BDA fibers and retrogradely labeled FG neurons of the PBP (Fig 2; S2-S3). This finding supports the above-mentioned observations and pointed to the caudal VTA as an interface through which the cerebellum would regulate prefrontal activity and striatal function. Projections from the lateral nucleus seemed to be glutamatergic and contacted TH+ cells and TH- within the VTA (Fig. 2; S2-S3).

A lesion in lobule VIII increases neural activity and PNNs expression in the lateral nucleus.

Student's t-tests revealed that the lesion of the vermis did not significantly change the cFos expression in the interpositus nucleus, either anterior (IntA) [t (10) = 1.48, p = 0.1697] or posterior (IntP) [T (10) = 2.04, p = 0.069] (Fig. 2B). Neither PNN expression in the IntA (p = 0.3384) nor in the IntP (p = 0.5832) were affected by the lesion. Under control conditions, neural activity in the Lat nucleus and PNN expression seem to be lower than in the IP nucleus. However, it is remarkable that the lesion in the posterior

vermis increased cFos [t (10) = 2.59, p = 0.0266] and WFA intensity [t (10) = 2.61, p = 0.0259] in the Lat (Fig. 3).

A lesion of lobule VIII in the vermis increases neural activity and PNN expression in the medial prefrontal cortex.

Then, we explored the impact of the cerebellar lesion on neural activity (cFos), DAT expression and PNN expression in the mPFC. As shown in figure 4, the cerebellar lesion increased cFos expression in both the IL [F (2,15) = 12.23, p = 0.0007] and PL [F (2,15) = 13.4, p = 0.0005] subdivisions of the mPFC. In the IL cortex, Tukey tests showed higher number of cFos+ neurons in the QA group as compared to the sham (p = 0.004) and Unp (p = 0.0009) groups. The number of cFos+ neurons also increased significantly in the PL region of the lesioned rats as compared to the sham (p = 0.0018) and Unp (p = 0.0008) groups. We did not observe significant differences in the expression of DAT in prefrontal regions among groups [IL: F (2,15) = 1.57, p = 0.2402; PL: [F (2,15) = 0.84, p = 0.4511] (Fig. 4S).

The cerebellar lesion enhanced WFA intensity in PNNs around PRV positive interneurons either in the IL [F (2,15) = 18.03, p = 0.0001] or the PL [F (2,15) = 7.262, p = 0.0062] cortices. Post hoc tests indicated that prefrontal PNNs were stronger in lesioned animals as compared to the sham [IL (p = 0.0006); PL (p = 0.0108)] and Unp [IL (p = 0.0002); PL (p = 0.0151)] groups (Fig. 4). The total number of PNNs in the mPFC was not affected by the cerebellar lesion [IL: F (2,15) = 0.24, p = 0.7897; PL: F (2,15) = 0.005, p = 0.9951] (Fig. 5S). However, the percentage of activated neurons (cFos+) surrounded by a PNN increased in the IL cortex [H (3) = 10.56, p = 0.0014] but not in the PL cortex [H (3) = 4.43, p = 0.1077]. Mann-Whitney tests revealed that such increase was an effect of the cerebellar lesion since lesioned rats showed higher number of interneurons positive for WFA and cFos than sham animals (p = 0.0449) or those of the Unp group (p = 0.0062)

(Fig. 5S). Moreover, the percentage of PRV positive interneurons that was activated and expressed a strong PNN (WFA+/PRV+/cFos+) increased after the lesion in the IL cortex [H (3) = 9.56, p = 0.0036] but not in the PL cortex [H (3) =1.17, p = 0.5782] (Fig. 5S).

Higher neural activity in the NAc and striatum after the lesion of lobule VIII.

Additionally, Student's t-test for independent samples showed that the cerebellar lesion elevated cFos expression in the Nac, dorsomedial striatum (DMS) and dorsolateral striatum (DLS) as compared to the sham group [nucleus accumbens core (NAcC) (t (10) = 3.48, p = 0.0059); shell (NAcSh) (t (10) = 5.06, p = 0.0005); dorsomedial striatum (DMS) (t (10) = 2.68, p = 0.0233); and the dorsolateral striatum (DLS) (t (10) = 4.76, p = 0.0008)]. However, the ventrolateral striatum (VLS) was unaffected by the cerebellar lesion (VLS) [T (10) = 1.53, p = 0.158]. (Fig. 5).

DISCUSSION

The present research is aimed at providing an explanatory model for the facilitative effect of a lesion in the dorsal region of the posterior vermis on cocaine-induced conditioned memory. First, we found a direct projection from the lateral nucleus to the VTA that also receives Purkinje axons from lobule VIII in the vermis. This pathway appears to be glutamatergic and contacts to dopaminergic and non-dopaminergic neurons within the VTA. Hypothetically, the activation of this DCN-VTA monosynaptic pathway could control activity of the cortico-striatal circuitry through dopaminergic and non-dopaminergic mechanisms.

Second, our findings indicate that damage in lobule VIII induces general disinhibition in the mPFC and striatal subdivisions that receive dopaminergic projections mainly from the VTA. To

estimate whether the cerebellar lesion might increase dopaminergic activity, we evaluated DAT expression in the mPFC. We observed high levels of DAT in the mPFC but, against our expectations, this expression was not affected by the lesion of the vermis. Nevertheless, the present results do not entirely rule out the possibility of increased VTA activity as an effect of the cerebellar lesion. All groups of rats were treated with the same cocaine regimen and thereby cocaine-induced DAT inhibition might occlude changes in VTA neuronal firing.

The idea of a cerebellar modulation of VTA has been grounded in a few previous findings which described indirect cerebellar-VTA pathways (47, 48), as well as direct control of the cerebellum onto the VTA (9, 22). Indeed, the cerebellum could reach the VTA through the reticulotegmental and pedunculopontine nuclei (47) and the mediodorsal and ventrolateral thalamus (48). More importantly, there is a direct cerebellar-VTA pathway (22), whose functional properties have been recently delineated in an elegant study (9). The optogenetic stimulation of the cerebellar-VTA pathway increases firing in one third of VTA neurons in vivo, eliciting excitatory synaptic currents, and inducing strong place preference for the location in which mice receive the optogenetic stimulation of the cerebellar projection (9). Moreover, the optogenetic stimulation of the cerebellar axons is as rewarding as the direct optogenetic activation of dopaminergic neurons in the VTA (9).

Third, our results also show that impairment of the posterior vermis induces an upregulation of PNN expression, as revealed by WFA fluorescence and higher levels of activity around parvalbumin positive interneurons in the mPFC. The fact that a small lesion in the posterior vermis is able to induce increased PNNs in the mPFC is remarkable. PNNs have been proposed as one of the mechanisms for the stabilization of drug-induced memories (36). Interestingly, previous findings demonstrate that both drug-induced conditioned preference (35) and drug self-administration (49-51) increase PNN

expression in the cerebellum and different prefrontal areas, respectively. Furthermore, PNN digestion within the PL cortex (50) and the anterior lateral hypothalamus (49) prevented the expression of cocaine-induced conditioned place preference and cocaine self-administration. The present data suggest that the cerebellar lesion could facilitate the acquisition of cocaine-cue associations and strengthen drug-induced memories by increasing synaptic stabilization mechanisms in the mPFC.

To our mind, the major contribution of the present research is to propose an explanatory hypothetical model for the function of the posterior cerebellar vermis on drug-related memory. In this model that integrate our results with those previously published (9), damage of the posterior dorsal vermis would release striatum-cortical networks from the inhibitory tonic control exerted by the cerebellum over the VTA, thereby promoting drug conditioning (Figure 6). The model may help to explain why patients with lesions or diseases affecting the posterior cerebellum presented difficulties in controlling their behavior and emotions (52). Moreover, our model predicts that the stimulation of the posterior cerebellar vermis would reduce drug-related effects and improve behavioral inhibition (Figure 6). Nevertheless, one crucial question for future research is to establish which functional characteristics and connectivity patterns make the dorsal region of lobule VIII in the vermis of special relevance to regulate DCN outputs to the VTA.

In summary, the present results indicate that: (1) the posterior cerebellar cortex may exert inhibitory control over the striatum and mPFC; (2) the Lat nucleus is the main efferent pathway relaying the cerebellar cortex processing to modulate activity and plasticity in the prefrontal-striatal network; and (3) the VTA could be a candidate to mediate cerebellar modulation on activity and plasticity in prefrontal-striatal loops that in turn can regulate cocaine-related behavior.

ACKNOWLEDGMENTS

This research was supported by the following grants and fellowships: Ministerio de Educación Cultura y Deporte (FPU12/04059); Universitat Jaume I (PREDOC2014/11); UJI (14I307.01/1); Ministerio de Economía y Competitividad (MINECO) (PSI2015-68600-P); and Plan Nacional de Drogas 2017 (PND-132400); Beca del Consejo Nacional de Ciencia y Tecnología (CONACyT- 575913).

English language editing was carried out by LanguageWire (LanguageWire Ltd | 12-15 Bermondsey Square | SE1 3UN | London, United Kingdom).

Authors acknowledge the constructive criticism from Kamran Khodakhah and Saleem Nicola to the present manuscript.

AUTHOR DISCLOSURE

All authors declare no conflicts of interest.

AUTHORSHIP

All authors made a notable contribution to the manuscript, and they were involved in critically revising the present version. Isis Gil-Miravet performed the stereotaxic surgeries and behavioral experiments; Isis Gil-Miravet and Francisco Olucha-Bordonau performed the tracing study; Isis Gil-Miravet, Edgar Arias de Saavedra-Sandoval, Ignacio Melchor-Eixea, and Lizbeth Vásquez-Celaya were involved in image and data analysis. Finally, Marta Miquel designed the study, supervised the surgeries and behavioral experiments, was involved in data analysis, and drafted the manuscript. All authors approved the present version of the manuscript.

DATA ACCESSIBILITY

The database is available from the corresponding author upon request.

REFERENCES

1. Ball GG, Micco DJ, Berntson GG. Cerebellar stimulation in the rat: complex stimulation-bound oral behaviors and self-stimulation. Physiol Behav. 1974;13:123–7.

2. Corbett D, Fox E, Milner PM. Fiber pathways associated with cerebellar self-stimulation in the rat: a retrograde and anterograde tracing study. Behav Brain Res. 1982;6:167–84.

3. Schmahmann JD, Pandya DN. Anatomic organization of the basilar pontine projections from prefrontal cortices in rhesus monkey. J Neurosci. 1997;17:438–58.

4. Sacchetti B, Baldi E, Lorenzini CA, Bucherelli C. Differential contribution of some cortical sites to the formation of memory traces supporting fear conditioning. Exp Brain Res. 2002;146:223–32.

5. Turner BM, Paradiso S, Marvel CL, Pierson R, Boles Ponto LL, Hichwa RD, et al. The cerebellum and emotional experience. Neuropsychologia. 2007;45:1331–41.

6. Zhu L, Sacco T, Strata P, Sacchetti B. Basolateral amygdala inactivation impairs learning-induced long-term potentiation in the cerebellar cortex. PLoS One. 2011;6:e16673.

7. Watson TC, Becker N, Apps R, Jones MW. Back to front: cerebellar connections and interactions with the prefrontal cortex. Front Syst Neurosci. 2014;8:4.

8. Wagner MJ, Kim TH, Savall J, Schnitzer MJ, Luo L. Cerebellar granule cells encode the expectation of reward. Nature. 2017;544:96–100.

9. Carta I, Chen CH, Schott AL, Dorizan S, Khodakhah K. Cerebellar modulation of the reward circuitry and social behavior. Science. 2019;364:6424.

10. Stanton GB. Topographical organization of ascending cerebellar projections from the dentate and interposed nuclei in Macaca mulatta: An anterograde degeneration study. J Comp Neurol. 1980;190:699–731.

11. Ikai Y, Takada M, Shinonaga Y, Mizuno N. Dopaminergic and non-dopaminergic neurons in the ventral tegmental area of the rat project, respectively, to the cerebellar cortex and deep cerebellar nuclei. Neuroscience. 1992;51:719–728.

12. Bostan AC, Strick PL. The basal ganglia and the cerebellum: nodes in an integrated network. Nat Rev Neurosci. 2018;19:338–350.

13. Xiao L, Bornmann C, Hatstatt-Burklé L, Scheiffele P. Regulation of striatal cells and goal-directed behavior by cerebellar outputs. Nat Commun. 2018;9:3133.

14. Panagopoulos NT, Papadopoulos GC, Matsokis NA. Dopaminergic innervation and binding in the rat cerebellum. Neurosci Lett. 1991;130:208–212.

15. Middleton FA, Strick PL. Basal ganglia and cerebellar loops: Motor and cognitive circuits. Brain Res Rev. 2000;31:236–250.

16. Ichinohe N, Mori F, Shoumura K. A di-synaptic projection from the lateral cerebellar nucleus to the laterodorsal part of the striatum via the central lateral nucleus of the thalamus in the rat. Brain Res. 2000;880:191–197.

17. Middleton FA, Strick PL. Cerebellar Projections to the Prefrontal Cortex of the Primate. J Neurosci. 2001;21:700–712.

18. Hoshi E, Tremblay L, Féger J, Carras PL, Strick PL. The cerebellum communicates with the basal ganglia. Nat Neurosci. 2005;8:1491–1493.

19. Buckner RL, Krienen FM, Castellanos A, Diaz JC, Yeo BTT. The organization of the human cerebellum estimated by intrinsic functional connectivity. J Neurophysiol.

2011;106:2322–2345.

20. Sang L, Qin W, Liu Y, Han W, Zhang Y, Jiang T, et al. Resting-state functional connectivity of the vermal and hemispheric subregions of the cerebellum with both the cerebral cortical networks and subcortical structures. Neuroimage. 2012;61:1213–1225.

21. Chen CH, Fremont R, Arteaga-Bracho EE, Khodakhah K. Short latency cerebellar modulation of the basal ganglia. Nat Neurosci. 2014;17:1767–1775.

22. Watabe-Uchida M, Zhu L, Ogawa SK, Vamanrao A, Uchida N. Whole-Brain Mapping of Direct Inputs to Midbrain Dopamine Neurons. Neuron. 2012;74:858–873.

23. Miquel M, Toledo R, Garcia L, Coria-Avila G, Manzo J. Why Should We Keep the Cerebellum in Mind When Thinking About Addiction? Curr Drug Abus Rev. 2009;2:26–40.

24. Miquel M, Vazquez-Sanroman D, Carbo-Gas M, Gil-Miravet I, Sanchis-Segura C, Carulli D, et al. Have we been ignoring the elephant in the room? Seven arguments for considering the cerebellum as part of addiction circuitry. Neurosci Biobehav Rev. 2016;60:1–11.

25. Yalachkov Y, Kaiser J, Naumer MJ. Sensory and motor aspects of addiction. Behav Brain Res. 2010;207:215–222.

26. Callu D, Puget S, Faure A, Guegan M, El Massioui N. Habit learning dissociation in rats with lesions to the vermis and the interpositus of the cerebellum. Neurobiol Dis. 2007;27:228–237.

27. Anderson CM, Maas LC, Frederick B, Bendor JT, Spencer TJ, Livni E, et al. Cerebellar Vermis Involvement in Cocaine-Related Behaviors. Neuropsychopharmacology. 2006;31:1318–1326.

28. Bonson KR, Grant SJ, Contoreggi CS, Links JM, Metcalfe J, Weyl HL, et al. Neural Systems and Cue-Induced Cocaine Craving. Neuropsychopharmacology. 2002;26:376–386.

29. Fuentes P, Barrós-Loscertales A, Bustamante JC, Rosell P, Costumero V, Ávila C. Individual differences in the Behavioral Inhibition System are associated with orbitofrontal cortex and precuneus gray matter volume. Cogn Affect Behav Neurosci. 2012;12:491–8.

30. Grant S, London ED, Newlin DB, Villemagne VL, Liu X, Contoreggi C, et al. Activation of memory circuits during cue-elicited cocaine craving. Proc Natl Acad Sci USA. 1996;93:12040–5.

31. Schneider F, Habel U, Wagner M, Franke P, Salloum JB, Shah NJ, et al. Subcortical correlates of craving in recently abstinent alcoholic patients. Am J Psychiatry. 2001;158:1075–1083.

32. Moulton EA, Elman I, Becerra LR, Goldstein RZ, Borsook D. The cerebellum and addiction: Insights gained from neuroimaging research. Addict Biol. 2014;19:317–331.

33. Carbo-Gas M, Vazquez-Sanroman D, Aguirre-Manzo L, Coria-Avila GA, Manzo J, Sanchis-Segura C, et al. Involving the cerebellum in cocaine-induced memory: Pattern of cFos expression in mice trained to acquire conditioned preference for cocaine. Addict Biol. 2014;19:61–76.

34. Carbo-Gas M, Vazquez-Sanroman D, Gil-Miravet I, De las Heras-Chanes J, Coria-Avila GA, Manzo J, et al. Cerebellar hallmarks of conditioned preference for cocaine. Physiol Behav. 2014;132:24–35.

35. Carbo-Gas M, Moreno-Rius J, Guarque-Chabrera J, Vazquez-Sanroman D, Gil-

Miravet I, Carulli D, et al. Cerebellar perineuronal nets in cocaine-induced pavlovian memory: Site matters. Neuropharmacology. 2017;125:166–180.

36. Sorg BA, Berretta S, Blacktop JM, Fawcett JW, Kitagawa H, Kwok JCF, et al. Casting a Wide Net: Role of Perineuronal Nets in Neural Plasticity. J Neurosci. 2016;36:11459–11468.

37. Gil-Miravet I, Guarque-Chabrera J, Carbo-Gas M, Olucha-Bordonau F, Miquel M. The role of the cerebellum in drug-cue associative memory: functional interactions with the medial prefrontal cortex. Eur J Neurosci. 2018;1–10.

38. LaLumiere RT, Niehoff KE, Kalivas PW. The infralimbic cortex regulates the consolidation of extinction after cocaine self-administration. Learn Mem. 2010;17:168–175.

39. Lalumiere RT, Smith KC, Kalivas PW. Neural circuit competition in cocaine-seeking: Roles of the infralimbic cortex and nucleus accumbens shell. Eur J Neurosci. 2012;35:614–622.

40. Paxinos G, Watson C. The Rat Brain in Stereotaxic Coordinates. 4th ed. Acad Press: San Diego, CA; 1998.

41. Schindelin J, Arganda-Carreras I, Frise E, Kaynig V, Longair M, Pietzsch T, et al. Fiji: an open-source platform for biological-image analysis. Nat Methods. 2012;9:676–82.

42. Vazquez-Sanroman D, Carbo-Gas M, Leto K, Cerezo-Garcia M, Gil-Miravet I, Sanchis-Segura C, et al. Cocaine-induced plasticity in the cerebellum of sensitised mice. Psychopharmacology (Berl). 2015;232:4455–4467.

43. Vazquez-Sanroman D, Leto K, Cerezo-Garcia M, Carbo-Gas M, Sanchis-Segura C,

Carulli D, et al. The cerebellum on cocaine: Plasticity and metaplasticity. Addict Biol. 2015;20:941–955.

44. Witter L, Rudolph S, Pressler RT, Lahlaf SI, Regehr WG. Purkinje Cell Collaterals Enable Output Signals from the Cerebellar Cortex to Feed Back to Purkinje Cells and Interneurons. Neuron. 2016;91:312–319.

45. Kasanetz F, Mato S, Sepers M, Inserm OJM, Cedex B. Addiction and synaptic plasticity in the nucleus accumbens. Area. 2008;661:269–296.

46. Geisler S, Zahm DS. Afferents of the ventral tegmental area in the rat-anatomical substratum for integrative functions. J Comp Neurol. 2005;490:270–294.

47. Forster GL, Blaha CD. Pedunculopontine tegmental stimulation evokes striatal dopamine efflux by activation of acetylcholine and glutamate receptors in the midbrain and pons of the rat. Eur J Neurosci. 2003;17:751–762.

48. Rogers TD, Dickson PE, Heck DH, Goldowitz D, Mittleman G, Blaha CD. Connecting the dots of the cerebro-cerebellar role in cognitive function: Neuronal pathways for cerebellar modulation of dopamine release in the prefrontal cortex. Synapse. 2011;65:1204–1212.

49. Blacktop JM, Todd RP, Sorg BA. Role of perineuronal nets in the anterior dorsal lateral hypothalamic area in the acquisition of cocaine-induced conditioned place preference and self-administration. Neuropharmacology. 2017;118:124–136.

50. Slaker M, Churchill L, Todd RP, Blacktop JM, Zuloaga DG, Raber J, et al. Removal of Perineuronal Nets in the Medial Prefrontal Cortex Impairs the Acquisition and Reconsolidation of a Cocaine-Induced Conditioned Place Preference Memory. J Neurosci. 2015;35:4190–4202.

51. Vazquez-Sanroman DB, Monje RD, Bardo MT. Nicotine self-administration remodels perineuronal nets in ventral tegmental area and orbitofrontal cortex in adult male rats. Addict Biol. 2017;22:1743–1755.

52. Schmahmann JD, Sherman JC. The cerebellar cognitive affective syndrome. Brain. 1998;121:561–579.

LEGENDS

Figure 1. Synaptic connectivity in the Lat Nucleus between Purkinje terminals from lobule VIII and somas of projection neurons to the VTA Top panels: infusion points of FG into the VTA (left, blue) and BDA into the apical region of the vermis (right, red). BDA diffusion was found not only in the vermis but also throughout the hemispheres. Colocalization was only seen within the IntA and Lat nuclei. Bottom panels: A coronal section of the lateral nucleus (Lat) in which a synaptic contact between a Purkinje terminal from lobule VIII of the vermis (BDA+) and one output neuron in the Lat (FG+) is shown. White arrows indicate the FG+ soma and the BDA+ terminal. Purkinje puncta was identified by calbindin (CALB/green) and the GABA vesicular transporter (VGAT/purple). All confocal images were taken at 40x with 2.5x zoom. Scale bar 10 μm. Right top panel: Digital amplification of 300x.

Figure 2. Putative synaptic contacts between neurons from the Lateral Nucleus and TH+ somas in the VTA projecting to The IL cortex Top panels: Infusion points of FG into the IL cortex (left, blue) and BDA into the lateral nucleus (right, red). Colocalization was observed within the contralateral parabrachial pigmented nucleus of the VTA (PBP). Bottom panels: White arrows point at an example of close apposition between the terminal of a projection neuron from the Lat nucleus (BDA+) and one dopamine neuron in the VTA (FG+) identified as expressing tyrosine hydroxylase (TH/green). Vesicular glutamate transporter (VGLUT2/purple) was identified in the BDA+ puncta. All confocal images were taken at 40x with 2.5x zoom. Scale bar of 10 μm. Right top panel: Digital amplification of 300x.

Figure 3. Effect of an excitotoxic lesion in lobule VIII on cFos and PNN expression in the DCN cFos expression in the interpositus anterior (IntA) (A), posterior (IntP) (B), and in the lateral nucleus (Lat) nuclei (C). PNN expression in the IntA (D), IntP (E), and

in the Lat nucleus (F). The cerebellar lesion increased cFos and PNN expression in the Lat nucleus (n=6) as compared to the sham group (n = 6). Data are shown as mean ± SEM. Scatterplots were overlapped for each group (*p < 0.05). All confocal images were taken at 20x magnification. Scale bar 100 μm.

Figure 4. Effect of an excitotoxic lesion in lobule VIII of the vermis on cFos and PNN expression in the mPFC (A) Diagrams of the cannula locations. Schematic diagrams depicting the largest (grey) and smallest (black) diffusion areas in the apical region of lobule VIII in the vermis. The extent of the diffusion areas was assessed using light microscopy and camera lucida drawings. The cerebellar lesion was made before cocaine-induced conditioning training**.** Effect on cFos expression in (B) IL and (C) PL for the control (Sham) (n = 6), quinolinic acid (QA) (n = 6), and unpaired (Unp) (n = 6) groups. WFA intensity in PNNs in the IL (D) and PL (E) cortices for the Sham (n = 6), QA (n = 6), and Unp groups (n = 6). Right panels, representative microphotographs of cFos and PNNs (WFA+, red) in the IL and PL cortex. The cerebellar lesion increased cFos and PNN expression in both subdivisions of the mPFC. The lesion was ineffective in producing both effects when cocaine was randomly associated with the odor cues (Unp). Data are shown as mean ± SEM and individual scores (*p < 0.05; **p < 0.01; ***p < 0.001). All images on the right panels were taken at 20x magnification. Scale bar 100 μm.

Figure 5. Effect of an excitotoxic lesion in lobule VIII on cFos expression in several striatal regions and the nucleus accumbens Dorsomedial striatum (DMS), dorsolateral striatum (DLS), ventrolateral striatum (VLS), nucleus accumbens core (NAcC) and nucleus accumbens shell (NAcSh). Data are shown as mean ± SEM of the sham (n = 6) and QA groups (n = 6). The cerebellar lesion increased cFos expression in DMS, DLS, NAcC and NAcSh, but not in the VLS (*p < 0.05; ***p < 0.001). All images were taken at 20x magnification. Scale bar 100 μm.

Figure 6. A hypothetical neuroanatomical model for role of lobule VIII on drug-related memory. Left panel: The lesion of lobule VIII by increasing activity in the lateral nucleus might heighten glutamate release within the VTA and facilitate the release of DA in mPFC and striatal regions. The lesion would then release striatum-cortical networks from the inhibitory tonic control exerted by the cerebellar cortex over the VTA through the Lat Nucleus thereby promoting drug effects. Right panel: The model predicts that the stimulation of the posterior cerebellar vermis would reduce drug-related effects and improve behavioral inhibitory control.

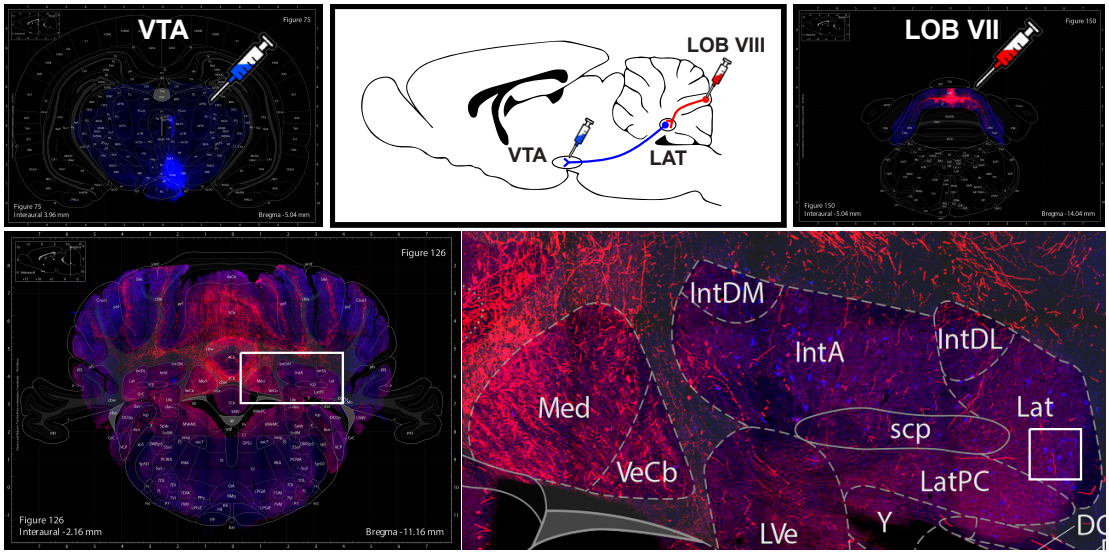
VTA
LOB VIII
VTA
LAT
LOB VII
Figure 126
Interaural -2.16 mm
Bregma -11.16 mm
IntDM
IntA
IntDL
Med
Lat
scp
VeCb
LatPC
LVe
Y

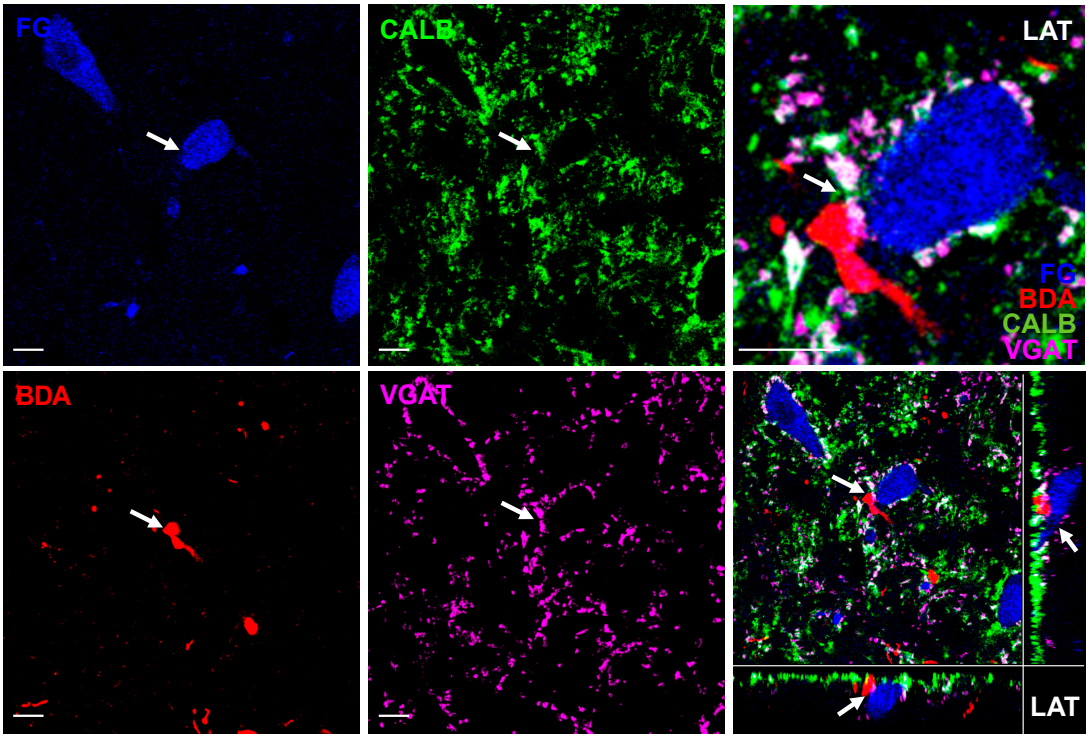
FG
CALB
LAT
FG
BDA
CALB
VGAT
BDA
VGAT
LAT

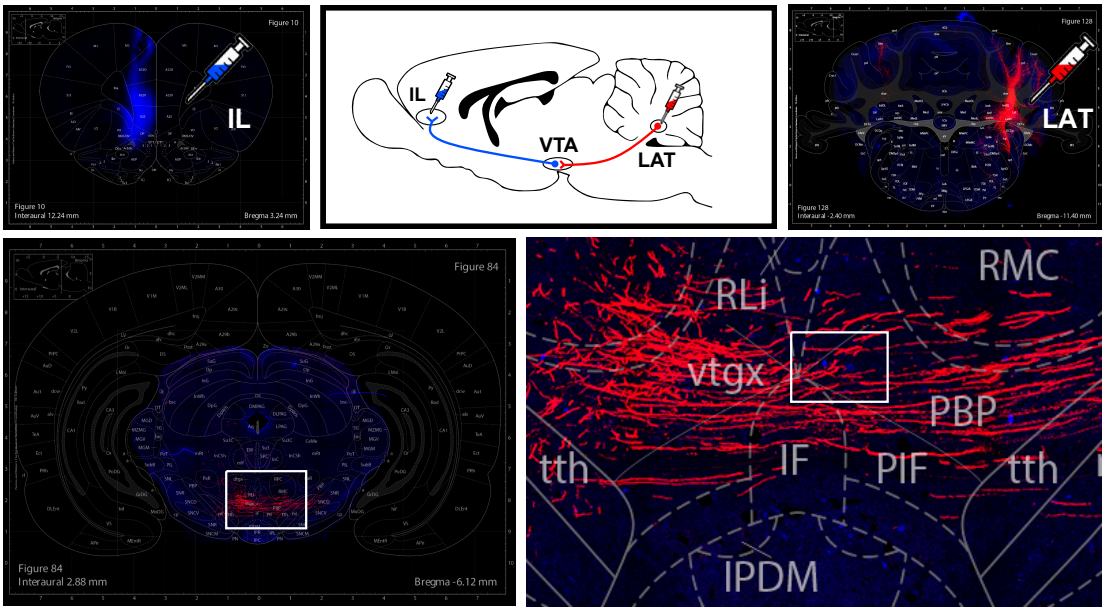
IL
VTA
LAT
LAT
Figure 84
Interaural 2.88 mm
Bregma -6.12 mm
RMC
RLi
vtgx
PBP
tth
IF
PIF
tth
IPDM

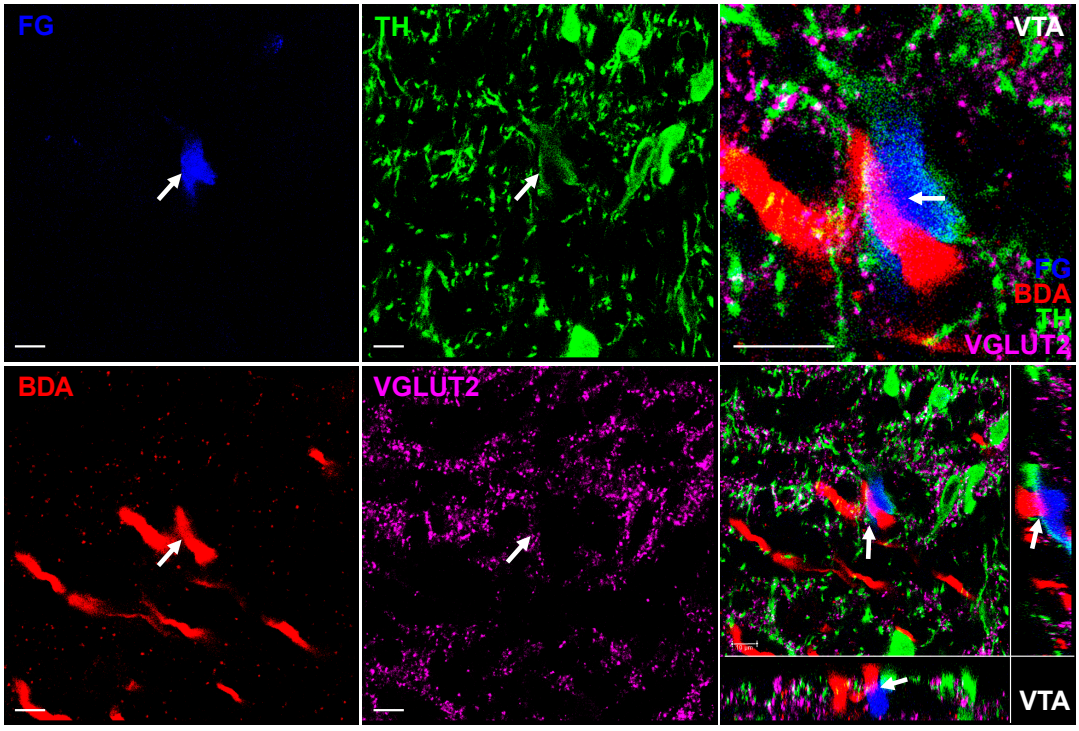
FG
TH
VTA
FG
BDA
TH
VGLUT2
BDA
VGLUT2
VTA

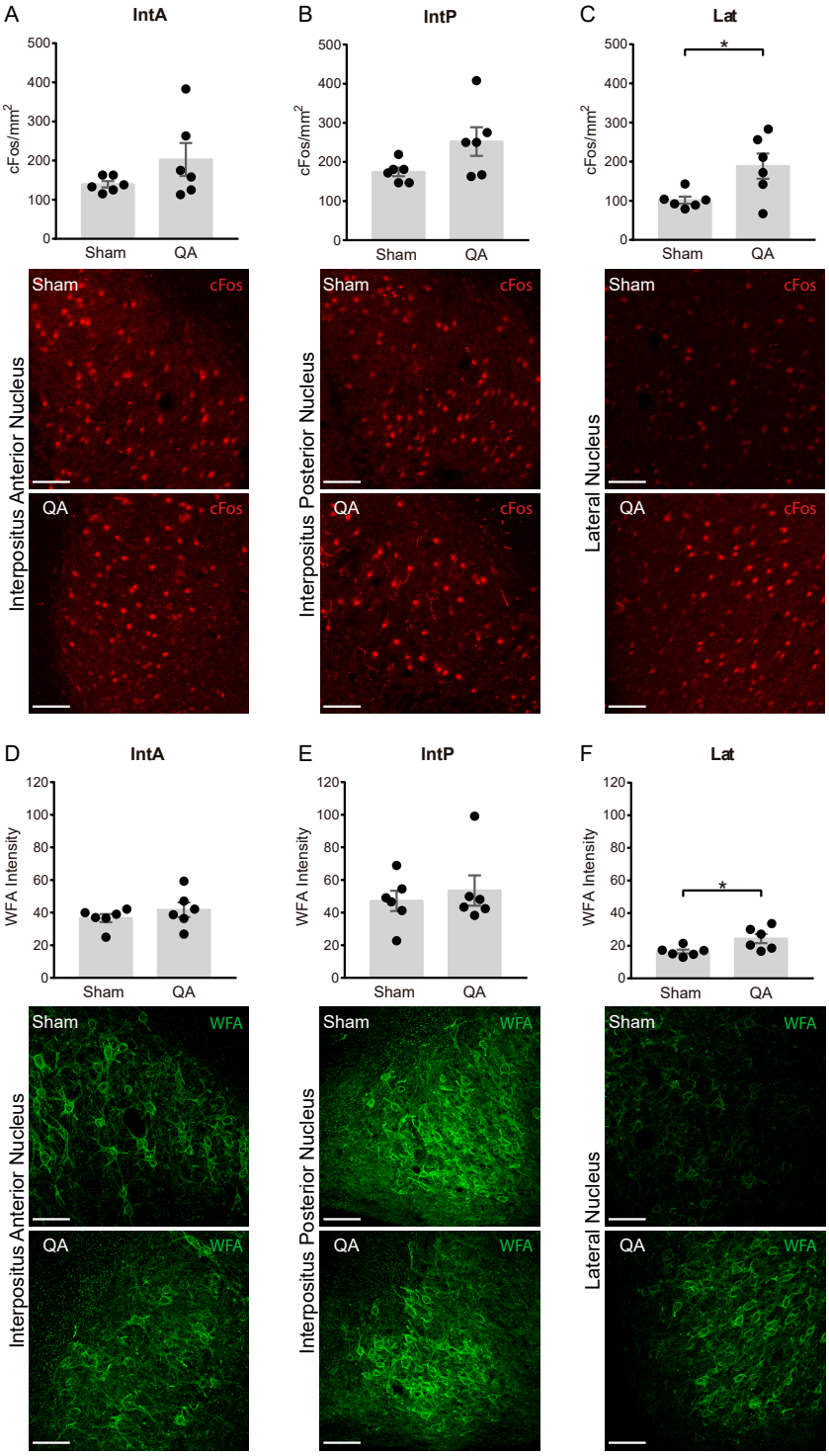
A
IntA
B
IntP
C
Lat
cFos/mm2
500
400
300
200
100
0
Sham
QA
*
Sham
cFos
QA
Interpositus Anterior Nucleus
Interpositus Posterior Nucleus
Lateral Nucleus
D
E
F
WFA Intensity
120
100
80
60
40
20
WFA

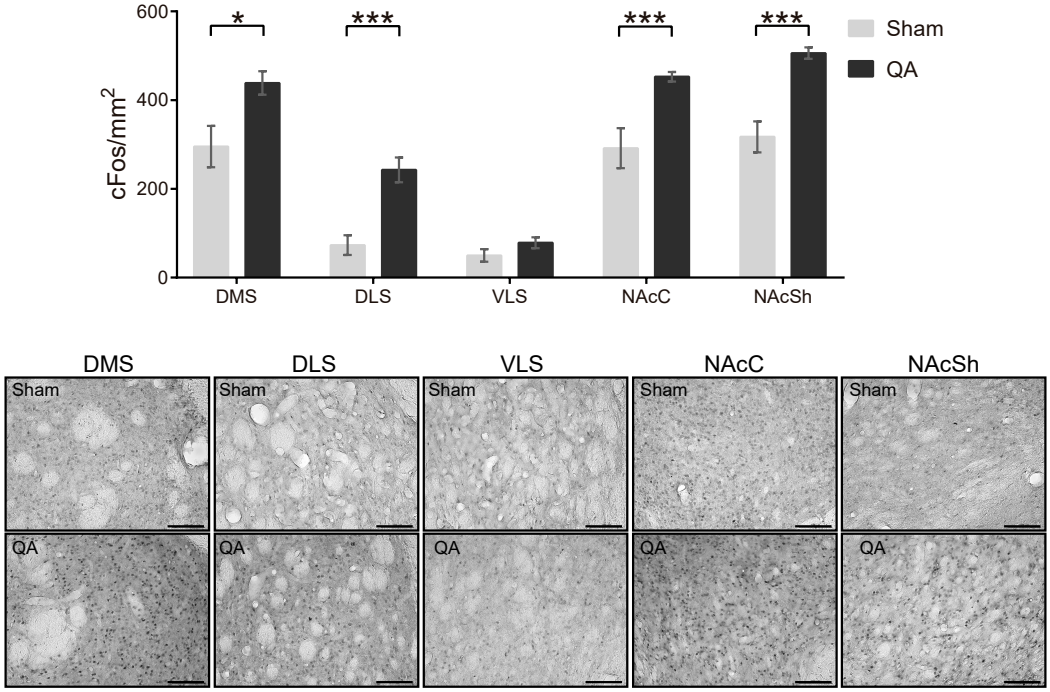
600
400
200
0
cFos/mm2
*
***
***
***
Sham
QA
DMS
DLS
VLS
NAcC
NAcSh
DMS
DLS
VLS
NAcC
NAcSh
Sham
QA

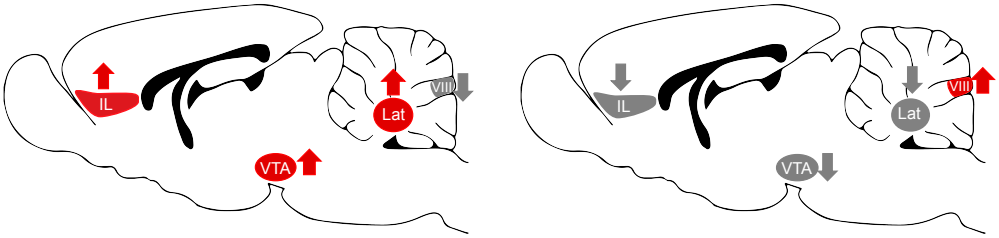
IL
Lat
VIII
VTA
IL
Lat
VIII
VTA

Supplementary information

Figure S1 Effect of a lesion in the apical region of lobule VIII on cocaine-induced conditioned preference. Quinolinic acid lesion were made before conditioning. Lesion Preference scores for the CS+ on the test day in the sham (n = 6), QA lesion (QA) (n = 6) and unpaired (Unp) (n = 6) groups. The QA lesion increased the proportion of rats that expressed cocaine-induced conditioned preference. Data are shown as individual preference scores overlaid mean ± SEM (*P < 0.05)

Figure S2 Infusions of BDA in the Lat nucleus (red) and FG in the IL cortex (blue). A coronal section of the VTA. White arrows indicate an example of a synaptic contact between the axon of a projection neuron from the Lat nucleus (BDA+) and one TH- neuron in the VTA (FG+) expressing VGLUT. All confocal images were taken a 40x and 2.5x zoom in a. Scale bar of 10 μm. Right panels: Digital amplification of 300x.

Figure S3 Infusions of BDA in the Lat nucleus (red) and FG in the IL cortex (blue). A coronal section of the VTA. White arrows indicate an example of a synaptic contact between the axon of a projection neuron from the Lat nucleus (BDA+) and one TH+ neuron (green) in the VTA (FG+) expressing Synapsin 1 in the presynaptic puncta (SYN/purple). All confocal images were taken a 40x and 2.5x zoom in a. Scale bar of 10 μm. Right panels: Digital amplification of 300x.

Figure S4 Effect of an excitotoxic lesion in lobule VIII on DAT expression. IL (A) PL (B). Dopaminergic terminals were identified as TH+. Data are shown as mean ± SEM of the sham (n = 6), QA (n = 6) and Unp (n = 6) groups. DAT expression did not change as an effect of the cerebellar lesion. All images were taken at 20x magnification. Scale bar 100 μm.

Figure S5 Perineuronal net expression in the mPFC after the cerebellar lesion. Top panels: Number of PNNs and PRV+ neurons in the IL (A-B) and PL (C-D) cortices. Bottom panels: Percentage of PRV+ (blue) activated (cFos+) (red) neurons that expressed a PNN (green) in the IL (E-F) and PL (G-H) cortices. Data are shown as median of the sham (n = 6), QA (n = 6) and Unp (n = 6) groups. The cerebellar lesion increased the number of activated GABA interneurons (PRV+) surrounding by a strong PNN. All images were taken at 20x magnification. Scale bar 100 μm.

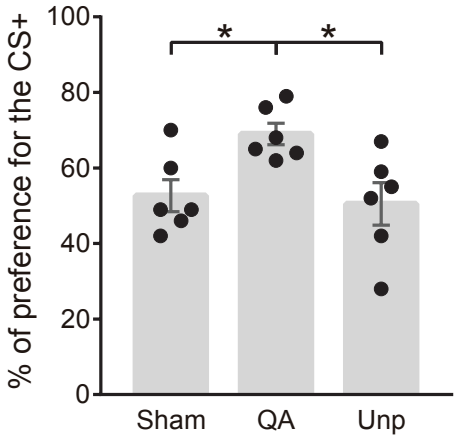
% of preference for the CS+
100
80
60
40
20
0
*
*
Sham
QA
Unp

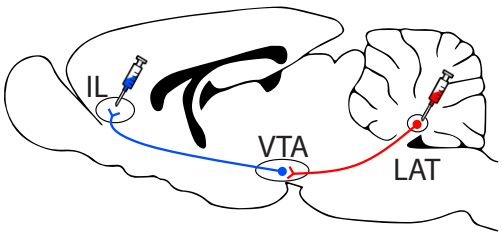
IL
VTA
LAT

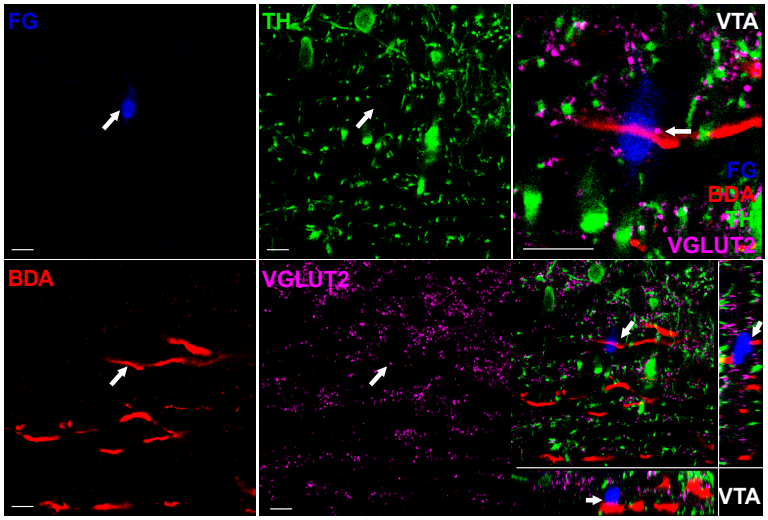
FG
TH
VTA
FG
BDA
VGLUT2
BDA
VGLUT2
VTA

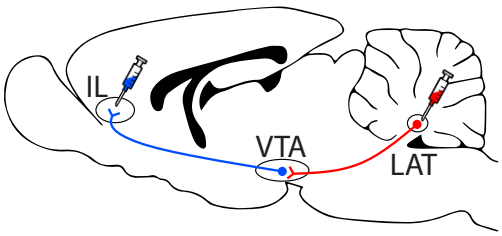
IL
VTA
LAT

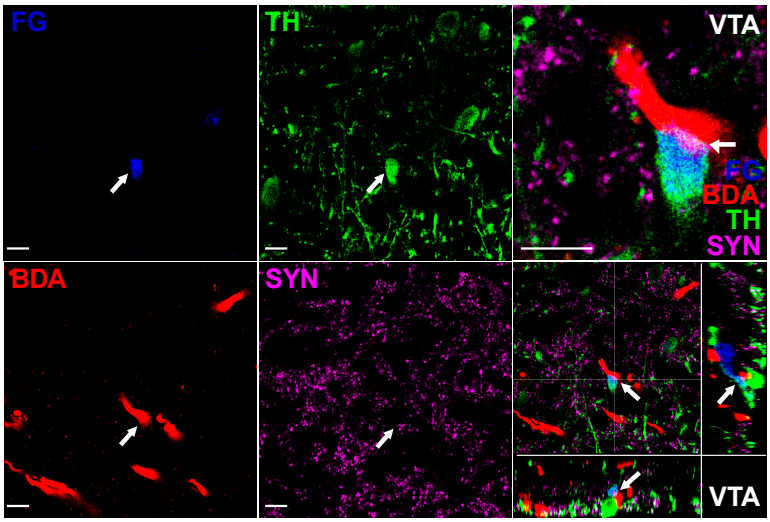
FG
TH
VTA
FG
BDA
TH
SYN
BDA
SYN
VTA

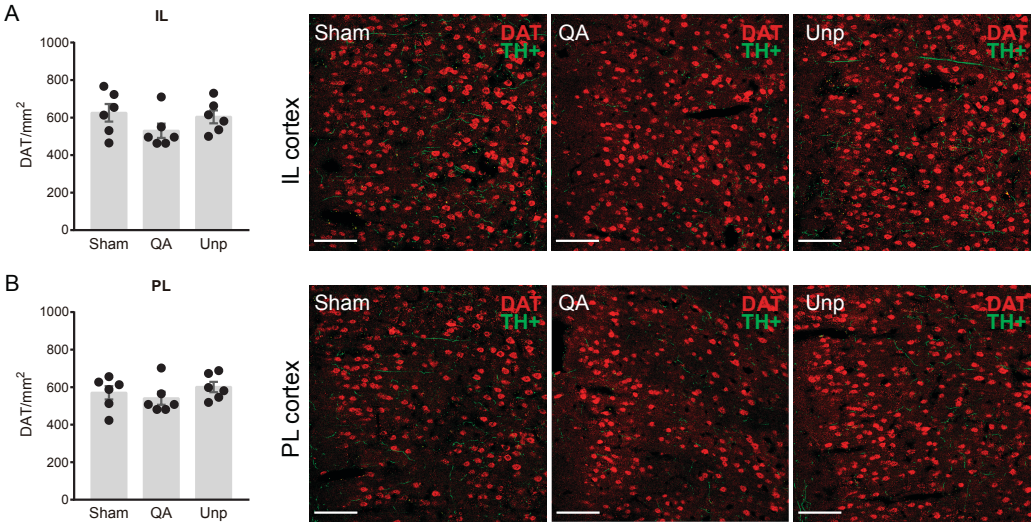
A
IL
DAT/mm2
1000
800
600
400
200
0
Sham
QA
Unp
B
PL
DAT/mm2
1000
800
600
400
200
0
Sham
QA
Unp
IL cortex
PL cortex
Sham
QA
Unp
DAT
TH+

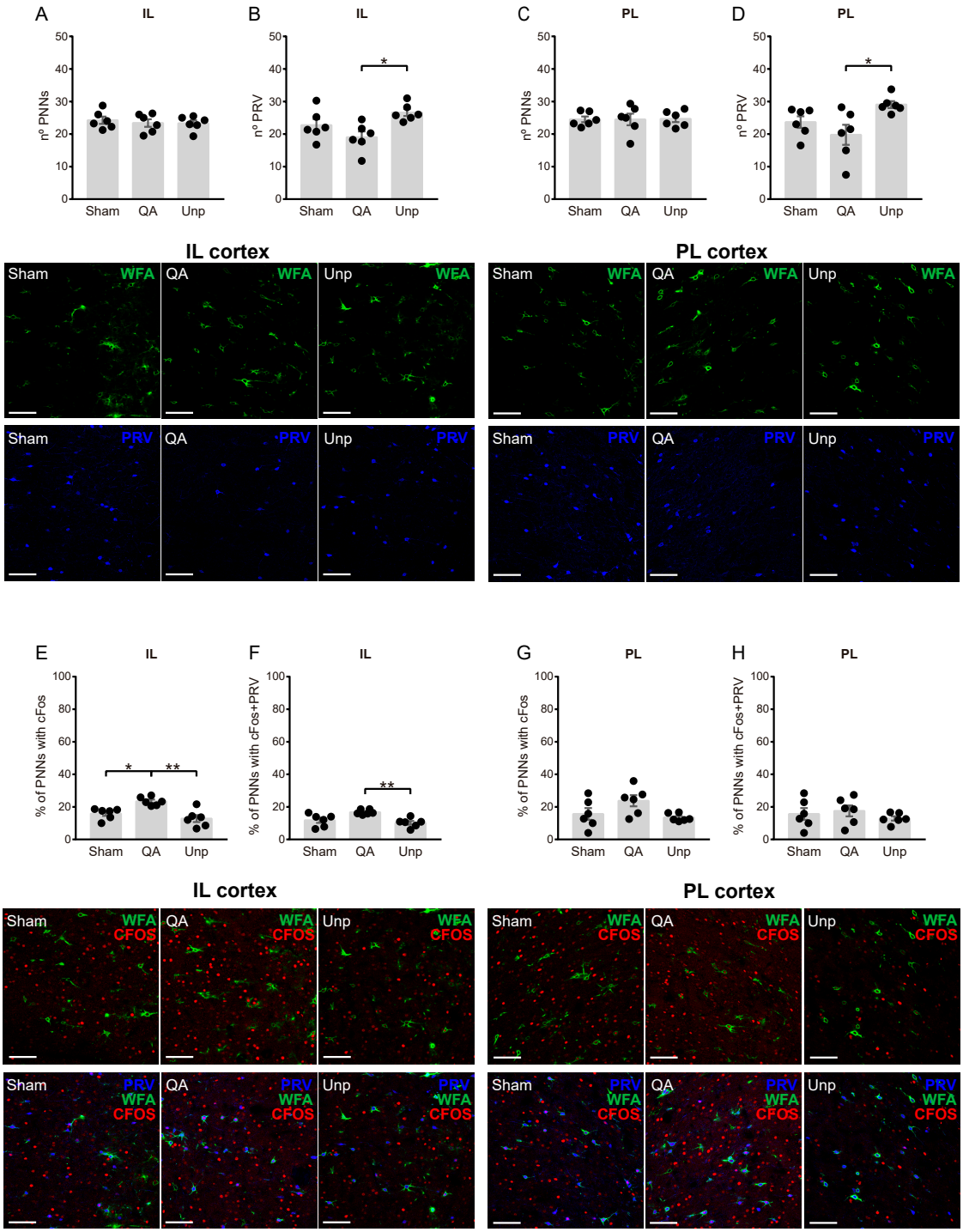
A
IL
nº PNNs
B
IL
nº PRV
C
PL
nº PNNs
D
PL
nº PRV
Sham
QA
Unp
IL cortex
PL cortex
WFA
PRV
E
IL
% of PNNs with cFos
F
IL
% of PNNs with cFos+PRV
G
PL
% of PNNs with cFos
H
PL
% of PNNs with cFos+PRV
CFOS